

# Colorless Chlorophyll Catabolites in Senescent Florets of Broccoli (*Brassica oleracea* var. *italica*)

Matthias H. Roiser, Thomas Müller, and Bernhard Kräutler\*

Institute of Organic Chemistry and Center for Molecular Biosciences, University of Innsbruck, Center of Chemistry and Biomedicine, Innrain 80/82, A-6020 Innsbruck, Austria

## Supporting Information

**ABSTRACT:** Typical postharvest storage of broccoli (*Brassica oleracea* var. *italica*) causes degreening of this common vegetable with visible loss of chlorophyll (Chl). As shown here, colorless Chl-catabolites are generated. In fresh extracts of degreening florets of broccoli, three colorless tetrapyrrolic Chl-catabolites accumulated and were detected by high performance liquid chromatography (HPLC): two “nonfluorescent” Chl-catabolites (NCCs), provisionally named *Bo*-NCC-1 and *Bo*-NCC-2, and a colorless 1,19-dioxobilin-type “nonfluorescent” Chl-catabolite (DNCC), named *Bo*-DNCC. Analysis by nuclear magnetic resonance spectroscopy and mass spectrometry of these three linear tetrapyrroles revealed their structures. In combination with a comparison of their HPL-chromatographic properties, this allowed their identification with three known catabolites from two other brassicacea, namely two NCCs from oil seed rape (*Brassica napus*) and a DNCC from degreened leaves of *Arabidopsis thaliana*.

**KEYWORDS:** broccoli, chlorophyll catabolites, structure elucidation, natural product, nutrition, vegetable

## INTRODUCTION

Breakdown of chlorophyll (Chl) is the visible symptom of leaf senescence<sup>1,2</sup> and is often also observable in ripening fruit.<sup>3</sup> Identification of the colorless tetrapyrrolic Chl-catabolite *Hv*-NCC-1 (Figure 1) from the monocot barley (*Hordeum vulgare*) opened up the field of Chl-breakdown to further structure-based studies.<sup>4</sup> Various “nonfluorescent” Chl-catabolites

(NCCs) have been found in senescent leaves.<sup>5–8</sup> NCCs have also been detected in ripening fruit, e.g., in apples and pears, and are excellent antioxidants.<sup>9</sup>

So far, over a dozen each of structurally different natural NCCs<sup>4,8</sup> and “fluorescent” Chl-catabolites (FCCs)<sup>8,10,11</sup> have been identified in leaf extracts, as well as a series of dioxobilin-type NCCs (DNCCs),<sup>8,12</sup> formerly called urogenobilinoidic Chl-catabolites (UCCs).<sup>13</sup> These three types of colorless catabolites show characteristic structural differences of their tetrapyrrolic bilin-type skeletons.<sup>12,14</sup> Knowledge of the tetrapyrrolic catabolites of Chl, collectively named “phyllobilins”,<sup>8,12</sup> has meanwhile provided a solid structural foundation for basic insights into Chl-breakdown.<sup>7,8</sup> Blue fluorescent FCCs are intermediates in Chl-breakdown that (typically) are only fleetingly existent as the direct biosynthetic precursors of the corresponding NCCs.<sup>15</sup> In contrast, the latter often accumulate in senescent leaves and have been described as “final” Chl-degradation products.<sup>6</sup> DNCCs are formally derived from NCCs by oxidative loss of their characteristic formyl group<sup>13</sup> and thus have also been called nor-NCCs.<sup>16</sup> However, as was shown recently in *Arabidopsis thaliana*, DNCCs are likely to arise via an enzyme-catalyzed deformylation of FCCs by a cytochrome P-450 enzyme.<sup>17</sup>

During postharvest storage, vegetables may degreen and their Chl is broken down. Thus, the problem of keeping harvested vegetables fresh and green relates directly to the visible phenomenon of Chl-breakdown.<sup>18,19</sup> Postharvest degreening in broccoli (*Brassica oleracea* var. *italica*) is of considerable interest<sup>18,20–27</sup> as it is in other vegetables.<sup>19,28,29</sup> Broccoli is a

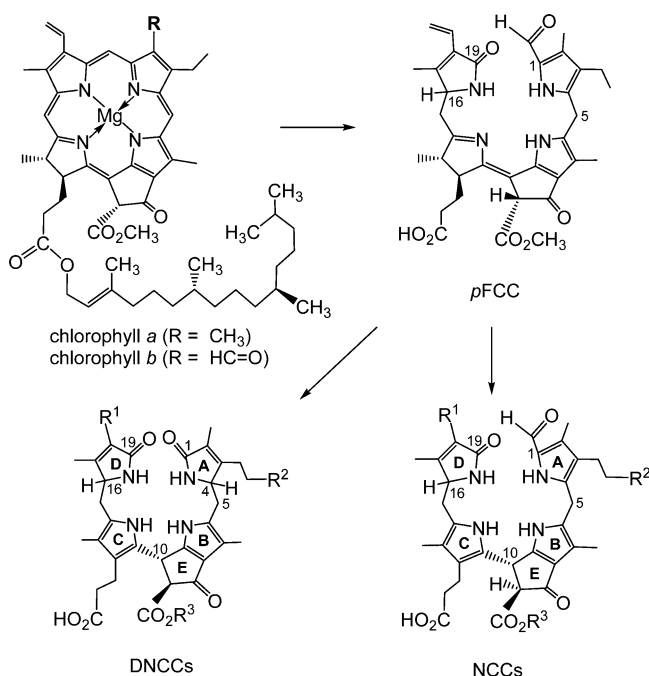


**Figure 1.** Short general structural overview of Chl-breakdown in senescent higher plants (for more details, see refs 7,8).

**Received:** November 18, 2014

**Revised:** January 21, 2015

**Accepted:** January 24, 2015

**Published:** January 24, 2015

popular vegetable in most parts of the world, and it enjoys considerable commercial interest.<sup>30</sup> The prevention or delay of postharvest degreening of broccoli has been addressed in various studies.<sup>18,26</sup> Surprisingly, the nature of the breakdown products of Chl in such a common vegetable is unknown. Identification of Chl-breakdown products may thus be of specific interest from a nutritional point of view, as some Chl-catabolites are suspected to possibly provide health benefits.<sup>9</sup> Earlier work from this group on naturally degreening leaves of spinach (*Spinacia oleracea*) has already addressed the question of the nature of Chl-catabolites in another vegetable.<sup>31,32</sup> As now reported here, we have analyzed degreened florets of broccoli and have identified three main Chl-catabolites in this vegetable, whose structures were elucidated.

## MATERIALS AND METHODS

**Chemicals and Plant Materials.** *Chemicals.* Acetone and methylene chloride ( $\text{CH}_2\text{Cl}_2$ , reagent-grade, commercial) were distilled before use for extractions. HPLC grade HiPerSolv CHROMANORM methanol (MeOH) was from VWR PROLABO. Potassium dihydrogen phosphate and potassium phosphate dibasic anhydrous were from Sigma-Aldrich. Sep-Pak-C18 Cartridges were from Waters Associates. The pH values were measured with a WTW Sentix21 electrode connected to a WTW pH535 digital pH meter.

*Plant Material.* Fresh, green broccoli (*Brassica oleracea* var. *italica*), produced by Conzorzio APO-FOGGIA S.C., Italy, was typically harvested 5 days before it was sold at the store (Spar Supermarket) in Innsbruck.

**Spectroscopy.** UV/vis: Hitachi U3000 spectrophotometer,  $\lambda_{\text{max}}$  [nm] (relative  $\epsilon$ ), in  $\text{H}_2\text{O}$ . CD: Jasco J715 spectropolarimeter,  $\lambda_{\text{max}}$  and  $\lambda_{\text{min}}$  [nm] ( $\Theta$ ), in  $\text{H}_2\text{O}$ .  $^1\text{H}$  nuclear magnetic resonance (NMR): Bruker UltraShield 600 MHz or Varian Unity Inova 500 MHz spectrometers,  $\delta$ [ppm] with  $\delta(\text{HDO}) = 4.79$  ppm, in  $\text{D}_2\text{O}$ . Electrospray ionization mass spectrometry (ESI-MS): Finnigan MAT 95S,  $m/z$  (rel. intensity), positive-ion mode, 1.4 kV spray voltage; signals with >5% rel. intensity are listed.

**High Performance Liquid Chromatography (HPLC).** Dionex P680 HPLC pump, online UV/vis-spectra: Dionex UVD340U. Column: Phenomenex HyperClone  $5\ \mu\text{m}$  ODS 250 mm  $\times$  4.6 mm i.d., column at 20  $^\circ\text{C}$ , protected with a Phenomenex ODS 4 mm  $\times$  3.0 mm i.d. precolumn was used with a flow rate 0.5 mL $\cdot\text{min}^{-1}$ . Solvent A: 50 mM aqueous potassium phosphate buffer (pH 7). Solvent B: MeOH, HPLC grade; solvent composition 1:0–5 min, A/B = 80/20; 5–55 min, A/B = 80/20 to 30/70, constant gradient; 55–60 min, 30/70 to 0/100, constant gradient; 60–70 min, A/B = 0/100; 70–75 min; A/B = 0/100 to 80/20, constant gradient. Analytical HPLC: sample size 50  $\mu\text{L}$ . Semipreparative HPLC: sample size 2 mL.

**Preparation and Storage of the Plant Material.** Using freshly bought broccoli, green broccoli florets were separated from the stem, their weight was determined, and they were stored up to 6 days at room temperature (about 22  $^\circ\text{C}$ ), either in the dark or in diffuse day light. On the day of the purchase and on the subsequent 6 days of storage, photographs of the broccoli florets documented their degreening (Figure 2). About 3–6% weight loss was determined at day 1 or day 6, respectively, presumably largely due to loss of water.

**Analysis of Chlorophylls and Chlorophyll Catabolites in Senescent Broccoli.** The content of Chl in extracts of broccoli florets was determined by an established UV/vis-analytical method.<sup>33</sup> The content of the Chl-catabolites was estimated by quantitative HPLC analysis of the extracts.

**Analysis of Chlorophylls.** The upper parts of broccoli florets (0.5–1.0 cm; i.e., typically 5–8 g, wet weight) were cut off and were stored for up to 6 days, either in darkness or exposed to diffuse day light. The fresh samples were collected in a mortar then suspended in 10 mL of acetone and ground at room temperature (reduced room light). The suspensions were filtered, and the remaining residues were extracted again with 10 mL of acetone. This procedure was repeated five times until the remaining plant material was practically colorless. Solvents

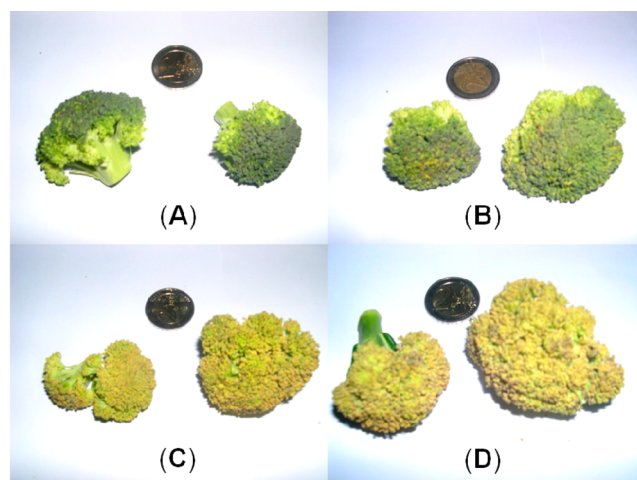


**Figure 2.** Photographic pictures of broccoli florets at various stages of degreening. (A) On day 1, (B) on day 3, (C) on day 5, and (D) on day 6 of the degreening experiment in the dark.

were removed from the collected green filtrates using a rotary evaporator, and green residues were obtained. These were dissolved in 50 mL of a mixture of 80% acetone and 20% 10 mM aqueous ammonium acetate buffer (pH 7); Chl was determined by UV/vis spectroscopy.<sup>33</sup>

**Analysis of Chlorophyll Catabolites.** For analysis of Chl-catabolites, samples of the upper 0.5–1 cm of broccoli florets roughly weighing 3.3 g were likewise collected in a mortar, frozen with liquid nitrogen, crushed, and extracted three times with 3 mL (each) of MeOH. The combined methanolic extracts were mixed 1/1 (v/v) with 50 mM aqueous potassium phosphate buffer (pH 7) and then subjected to analytical HPLC. The catabolites were characterized spectroscopically as described below.

**Isolation and Structure Elucidation of Colorless Chlorophyll Catabolites.** For structure elucidation, Chl-catabolites were obtained from broccoli florets that were stored for 5 days at room temperature in the dark. The upper 0.5–1 cm of the yellow florets (76.72 g, total wet weight) were cut, frozen with liquid nitrogen, and crushed in a mortar. The cold samples were extracted three times with 100 mL each of MeOH. The combined methanolic extract was analyzed by HPLC (Figure 3) and was concentrated to near dryness under reduced pressure. The residue was taken up in 50 mL of aqueous potassium phosphate buffer (50 mM, pH = 5.1), and the solution was centrifuged (3000 rpm 5 min); a dark-green residue separated, which was extracted two times with 5 mL (each) of aqueous potassium phosphate buffer. The greenish aqueous phases were combined and extracted eight times with 50 mL (each) of  $\text{CH}_2\text{Cl}_2$ . Analyses of the now roughly 50 mL of slightly yellow aqueous phase by HPLC indicated the presence of two Chl-catabolites, of *Bo*-NCC-1 (1) and *Bo*-DNCC (3). The greenish organic phase contained the less polar *Bo*-NCC-2 (2) predominantly.

The greenish  $\text{CH}_2\text{Cl}_2$  phase was evaporated under reduced pressure, and the remaining residue was resuspended in 25 mL of potassium phosphate buffer (50 mM, pH = 7.0). From the supernatant, *Bo*-NCC-2 (2) was isolated by semipreparative HPLC. The fractions containing raw 2 were combined and purified by a second round of semipreparative HPLC. The combined fractions containing pure 2 were desalted by filtration through Sep-Pak-C18 cartridges. Removal of the solvents under reduced pressure gave a sample of *Bo*-NCC-2 (2) as an off-white residue that was dried under high vacuum. The sample of pure NCC 2 was dissolved in 0.5 mL of  $\text{H}_2\text{O}$ , and its amount was determined as 0.32  $\mu\text{mol}$  (194  $\mu\text{g}$ ) by UV analysis ( $\log \epsilon_{(315\text{ nm})} = 3.93$ ).<sup>32</sup>

The yellow aqueous phase that contained *Bo*-NCC-1 (1) and *Bo*-DNCC (3) was concentrated to about 10 mL using a rotatory evaporator. The now yellow–brownish solution was subjected to semipreparative HPLC in order to isolate raw *Bo*-NCC-1 (1) and *Bo*-

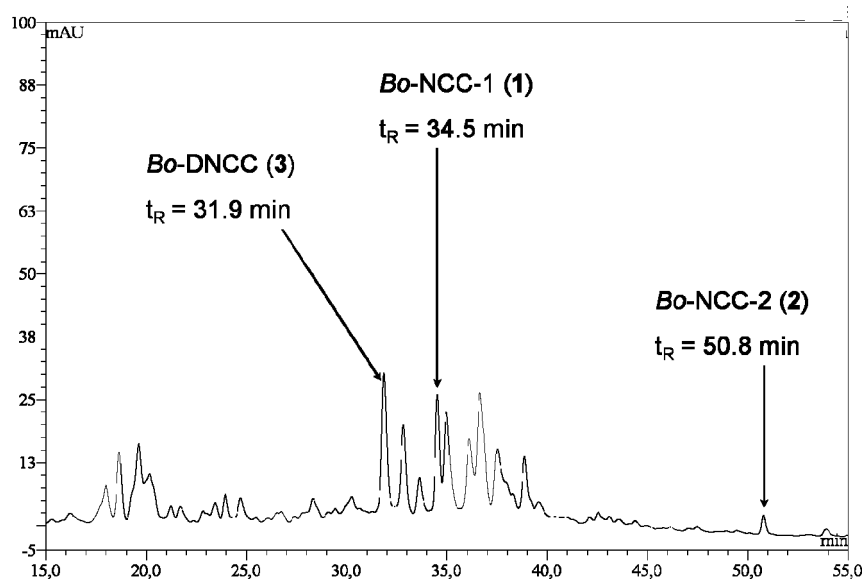


**Figure 3.** HPLC analysis of a methanolic extract of senescent broccoli florets (online detection at 250 nm). Fractions identified as Chl-catabolites by their UV/vis spectra, are labeled correspondingly as *Bo-NCC-1* (1), *Bo-NCC-2* (2), and *Bo-DNCC* (3).

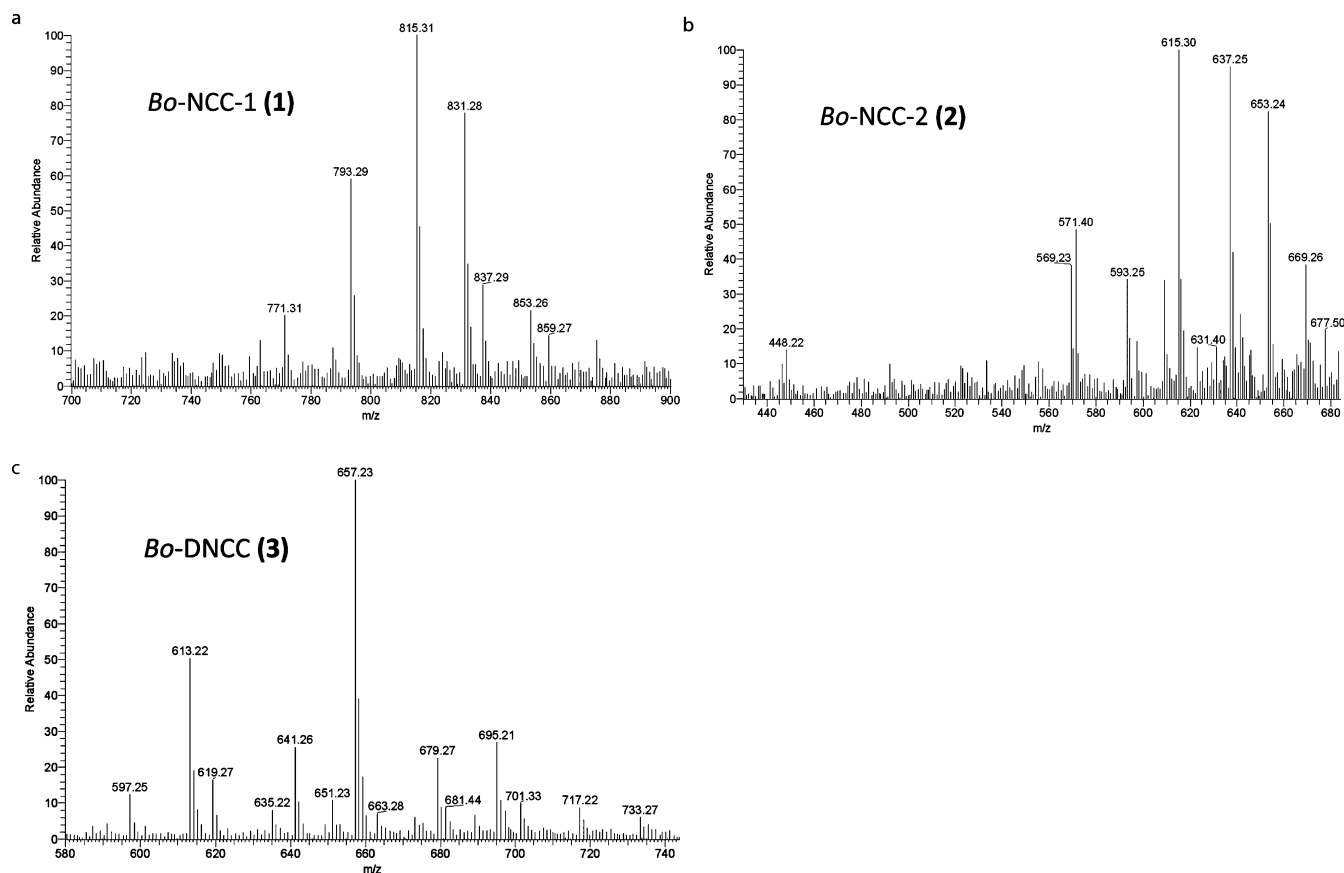


**Figure 4.** ESI-MS-spectra of *Bo-NCC-1* (1), *Bo-NCC-2* (2), and of *Bo-DNCC* (3).

DNCC (3). The isolated product fractions were purified by a second round of semipreparative HPLC. Fractions containing 1 or 3 were combined and desalted by filtration through Sep-Pak-C18 cartridges. Solvents were evaporated using a rotatory evaporator, furnishing off-white residues, which were dried at high vacuum, for further analysis. About 0.31  $\mu\text{mol}$  (244  $\mu\text{g}$ ) of NCC 1 were obtained (UV-analysis in  $\text{H}_2\text{O}^{32}$ ). The sample of the DNCC 3 was also analyzed by UV-

spectroscopy ( $\log \epsilon_{(237 \text{ nm})} = 4.49$ )<sup>16</sup> and was estimated to contain an amount of 0.25  $\mu\text{mol}$  (188  $\mu\text{g}$ ).

**Spectroscopic Data.** *Bo-NCC-1* (1). UV/vis ( $\lambda_{\text{max}}$  [nm], rel.  $\epsilon$ ): 240 (1.22), 250 (1.05), 319 (1.00). CD ( $\lambda_{\text{max}}$  and  $\lambda_{\text{min}}$  [nm],  $\Theta$ ): 228 (1.6), 245 (−5.3), 257 (−3.8), 282 (−15.0), 321 (8.1).  $^1\text{H}$  NMR (500 MHz in  $\text{D}_2\text{O}$ , at 293 K):  $\delta$  = 1.35 (s,  $\text{H}_3\text{C-17}^1$ ), 1.87 (s,  $\text{H}_3\text{C-13}^1$ ), 2.19 (s,  $\text{H}_3\text{C-2}^1$ ), 2.22 (s,  $\text{H}_3\text{C-7}^1$ ), 2.26 (m,  $\text{H}_2\text{C-12}^2$ ), 2.64 (m,  $\text{H}_2\text{C-12}^1$ ), 2.72 (m,  $\text{H}_2\text{C-3}^1$ ), 2.74 (m,  $\text{H}_\text{A}\text{-C-15}$ ), 2.86 (m,  $\text{H}_\text{B}\text{-C-15}$ ), 3.26 (t,



$J = 8.6$  Hz, HC-2'), 3.37 (m, HC-4'), 3.43 (m, HC-5'), 3.49 (t,  $J = 8.9$  Hz, HC-3'), 3.57 (m, H<sub>A</sub>C-3'), 3.59 (m, H<sub>2</sub>C-8'), 3.71 (m, H<sub>A</sub>C-6'), 3.72 (m, H<sub>B</sub>C-3'), 3.91 (m, H<sub>B</sub>C-6'), 3.97 (s, HC-16), 3.97 (m,  $J = 17.1$  Hz, H<sub>A</sub>C-5), 4.09 (m,  $J = 17.1$  Hz, H<sub>B</sub>C-5), 4.39 (d,  $J = 8.1$  Hz, HC-1'), 4.72 (m, HC-10, superimposed by signal of HDO), 5.42 (d,  $J_2 = 11.6$  Hz, H<sub>cis</sub>-C-18'), 5.83 (d,  $J_1 = 18.2$  Hz, H<sub>trans</sub>-C-18'), 6.29 (dd,  $J_1 = 18.0$  Hz  $J_2 = 12.2$  Hz, HC-18'), 9.15 (s, HC-20). ESI-MS:  $m/z$  (%) = 859.3 (7, [M - 2H + 3Na]<sup>+</sup>), 854.3 (11), 853.3 (21, [M - H + Na + K]<sup>+</sup>); 839.3 (9), 838.31 (11), 837.3 (29, [M - H + 2Na]<sup>+</sup>); 833.3 (16), 832.3 (44), 831.3 (76, [M + K]<sup>+</sup>); 818.3 (9) 817.3 (16), 816.3 (46), 815.3 (100, [M + Na]<sup>+</sup>); 795.3 (9), 794.3 (24), 793.3 (56, C<sub>40</sub>H<sub>49</sub>N<sub>4</sub>O<sub>13</sub> [M + H]<sup>+</sup>); 772.3 (4), 771.3 (16, [M - CO<sub>2</sub> + Na]<sup>+</sup>) (Figure 4).

**Bo-NCC-2 (2).** UV/vis ( $\lambda_{\max}$  [nm], rel.  $\epsilon$ ): 240 (1.23), 322 (1.00). CD ( $\lambda_{\max}$  and  $\lambda_{\min}$  [nm],  $\Theta$ ): 226 (-2.3), 244 (-15.6), 259 (-9.4), 282 (-26.8), 325 (18.5). <sup>1</sup>H NMR (600 MHz, in D<sub>2</sub>O, at 283 K): 0.87 (t,  $J = 7.55$  Hz, H<sub>3</sub>C-3'), 1.29 (s, H<sub>3</sub>C-17'), 1.85 (s, H<sub>3</sub>C-13'), 2.13 (s, H<sub>3</sub>C-2'), 2.21 (s, H<sub>3</sub>C-7'), 2.27 (m, H<sub>2</sub>C-12'), 2.37 (m, H<sub>2</sub>C-3'), 2.63 (m, H<sub>2</sub>C-12'), 2.68 (m, H<sub>A</sub>C-15), 2.86 (dd,  $J_1 = 14.73$  Hz  $J_2 = 5.79$  Hz, H<sub>B</sub>C-15), 3.88 (m, HC-1 H<sub>A</sub>C-5), 4.05 (m, H<sub>B</sub>C-5), 4.70 (m, HC-10), 5.42 (d,  $J_2 = 11.9$  Hz, H<sub>cis</sub>-C-18'), 5.82 (d,  $J_1 = 18.0$  Hz, H<sub>trans</sub>-C-18'), 6.28 (dd,  $J_1 = 18.0$  Hz  $J_2 = 11.9$  Hz, HC-18'), 9.10 (s, HC-20). ESI-MS:  $m/z$  (%) = 655.30 (16), 654.24 (48), 653.24 (79, [M + K]<sup>+</sup>); 639.20 (14), 638.13 (38), 637.25 (94, [M + Na]<sup>+</sup>); 617.39 (16), 616.28 (34), 615.30 (100, C<sub>34</sub>H<sub>39</sub>N<sub>4</sub>O<sub>7</sub> [M + H]<sup>+</sup>); 611.19 (7), 610.27 (15), 609.24 (32, [M - CO<sub>2</sub> + K]<sup>+</sup>); 594.20 (16), 593.25 (34, [M - CO<sub>2</sub> + Na]<sup>+</sup>); 572.27 (12), 571.40 (50, [M - CO<sub>2</sub> + H]<sup>+</sup>); 569.21 (36); 492.20 (10, [M - Ring D + H]<sup>+</sup>); 448.22 (14, [M - Ring D-CO<sub>2</sub> + H]<sup>+</sup>) (Figure 4).

**Bo-DNCC (3).** UV/vis ( $\lambda_{\max}$  [nm], rel.  $\epsilon$ ): 250 (1.00); 290 (broad, 0.2). CD ( $\lambda_{\max}$  and  $\lambda_{\min}$  [nm],  $\Theta$ ): 226 (8.6); 244 (0.6); 259 (-9.4); 282 (-26.8); 325 (18.5). <sup>1</sup>H NMR (600 MHz in D<sub>2</sub>O by 293 K): 1.68 (s, H<sub>3</sub>C-2'), 1.85 (s, H<sub>3</sub>C-13'), 1.92 (s, H<sub>3</sub>C-17'), 2.02 (s, H<sub>3</sub>C-7'), 2.13 (m, H<sub>2</sub>C-12'), 2.45 (m, H<sub>A</sub>C-3' H<sub>2</sub>C-12'), 2.61 (m, H<sub>A</sub>C-5 H<sub>A</sub>C-15), 2.76 (m, H<sub>B</sub>C-3'), 2.95 (dd,  $J_1 = 15.0$  Hz  $J_2 = 4.8$  Hz, H<sub>B</sub>C-15), 3.07 (dd,  $J_1 = 15.0$  Hz  $J_2 = 4.4$  Hz, H<sub>B</sub>C-5), 3.67 (m, H<sub>2</sub>C-3'), 4.18 (t,  $J = 6.0$  Hz, HC-16), 4.30 (m, HC-4), 4.60 (m, HC-10), 5.30 (d,  $J_2 = 11.8$  Hz, H<sub>cis</sub>-C-18'), 5.72 (d,  $J_1 = 17.9$  Hz, H<sub>trans</sub>-C-18'), 6.28 (dd,  $J_1 = 17.9$  Hz  $J_2 = 11.7$  Hz, HC-18'). ESI-MS:  $m/z$  (%) = 733.27 (6, [M - 2H + 3K]<sup>+</sup>); 718.19 (6), 717.22 (9, [M - 2H + Na + 2K]<sup>+</sup>); 701.33 (10, [M - 2H + 2Na + K]<sup>+</sup>); 697.20 (8), 696.18 (11), 695.21 (26, [M - H + 2K]<sup>+</sup>); 681.44 (8), 680.26 (8), 679.27 (22, [M - H + Na + K]<sup>+</sup>); 660.25 (6), 659.24 (18), 658.23 (49), 657.23 (100, [M + K]<sup>+</sup>); 651.23 (12, [M - H-CO<sub>2</sub> + 2K]<sup>+</sup>); 642.25 (10), 641.26 (25, [M + Na]<sup>+</sup>); 635.22 (8, [M - H-CO<sub>2</sub> + Na + K]<sup>+</sup>); 620.28 (8), 619.27 (16, C<sub>33</sub>H<sub>39</sub>N<sub>4</sub>O<sub>8</sub> [M + H]<sup>+</sup>); 615.23 (8), 614.22 (19), 613.22 (50, [M - CO<sub>2</sub> + K]<sup>+</sup>); 598.25 (5), 597.25 (13, [M - CO<sub>2</sub> + Na]<sup>+</sup>) (Figure 4).

**Identification of Bo-NCC-1, Bo-NCC-2, and Bo-DNCC with Known Chlorophyll Catabolites.** According to their spectroscopic data, Bo-NCC-1 (1), Bo-NCC-2 (2), and Bo-DNCC (3) had the same molecular constitutions as Bn-NCC-2 and Bn-NCC-4, two NCCs from oil seed rape (*Brassica napus*).<sup>34</sup> For the purpose of their further identification, the HPL-chromatographic behavior of Bo-NCC-1 (1) and of Bn-NCC-2 was compared, as well as that of Bo-NCC-2 (2) and of Bn-NCC-4. The samples from the two plant sources showed (pairwise) identical chromatographic properties. In a third coinjection experiment, Bo-DNCC (3) and a DNCC from *A. thaliana*, provisionally named At-DNCC-1,<sup>17</sup> also showed the same chromatographic behavior.

## RESULTS

Fresh green florets of broccoli (*Brassica oleracea* var. *italica*), which were bought in a super market, were stored in a dry place at ambient temperature for up to 6 days, either in the dark or being exposed to diffuse day light. In both cases, the broccoli florets degreened and developed a faint yellow color (Figure 2). At regular time intervals, a broccoli floret was selected and its upper part (about 3 g wet weight) was then analyzed. In the extracts obtained, residual Chl *a* and Chl *b* were analyzed by

UV/vis-spectroscopy, and three colorless Chl-catabolites were tentatively identified by HPLC analysis (Figure 3). In the green, commercially available broccoli florets, the here characterized three colorless Chl-catabolites were already present in small amounts. During storage (in darkness or diffuse day light), the Chl-content in broccoli was seen to decrease to about 50% within roughly 2 days. After 6 days, less than 10% of the original Chl was still present. In the broccoli florets, two NCC fractions were typified, and a DNCC, based on their characteristic UV absorbance properties. In both cases of storage, in the dark and in diffuse daylight, the amount of the most polar NCC, named Bo-NCC-1 (1), increased strongly until day 3 and decreased upon further storage. The lesser abundant and less polar NCC, Bo-DNCC (3) displayed a similar profile of its presence in the florets. A small amount of Bo-NCC-2 (2) was present from the first day onward with a trend to decrease during storage. Other relevant fractions with UV/vis spectral signatures of colorless Chl-catabolites were not found. During the first 2 days of storage, the observed accumulation of Chl-catabolites was estimated to come up for about 30–35%, overall, of the Chls lost due to the degreening process. As was noted elsewhere with respect to the content of Chl-catabolites,<sup>6</sup> storage of broccoli beyond the early stages of degreening and senescence also showed significantly decreased amounts of the recovered Chl-catabolites. Indeed, degradation of organic micronutrients (vitamins and secondary plant metabolites) during storage is a widely observed phenomenon.

For the purpose of isolation and structure analysis of Chl-catabolites, yellow broccoli florets were selected at day 5 of their storage in the dark, and the upper 0.5–1 cm was severed from the stalk, giving a sample of 76.7 g (wet weight), which was crushed and extracted with MeOH (as described in detail in the Materials and Methods section). After a two-stage isolation and purification procedure by HPLC, 0.32  $\mu$ mol (194  $\mu$ g) of Bo-NCC-2 (2), 0.31  $\mu$ mol (244  $\mu$ g) Bo-NCC-1 (1), and 0.25  $\mu$ mol (188  $\mu$ g) Bo-DNCC (3) were obtained.

The samples of the isolated three Chl-catabolites were used for structure determination. UV spectra allowed the classification of two NCCs<sup>4,6</sup> (1 and 2) and of a DNCC (3).<sup>13,16</sup> The UV-spectra of the NCC fractions 1 and 2 showed absorption maxima at 319 and at 322 nm, respectively, characteristic for the  $\alpha$ -formyl-pyrrole moiety (ring A) of NCCs.<sup>6,35</sup> The UV-spectrum of the Bo-DNCC (3) showed no maxima, but absorption bands near 250 and 290 nm, as is typical for 1,19-dioxobilane-type NCCs (DNCCs).<sup>13,16</sup> CD-spectra of the purified NCCs showed positive and negative extrema at 321 and at 282 nm, respectively, as is characteristic of natural NCCs.<sup>15,36</sup> The CD spectrum of Bo-DNCC (3) exhibited a very weak maximum at 310 nm, and a pronounced negative extremum at 282 nm, as was described similarly for At-DNCC-1,<sup>17</sup> suggesting the configuration at C15 to be the same as in the DNCC from *A. thaliana*.<sup>17</sup>

The molecular formula of Bo-NCC-1 (1) was deduced as C<sub>40</sub>H<sub>48</sub>N<sub>4</sub>O<sub>13</sub> from its electrospray ionization (ESI) mass spectrum (Figure 4), in which the pseudomolecular ions [M + H]<sup>+</sup> and [M + Na]<sup>+</sup> were found at  $m/z = 793.29$  and at  $m/z = 815.31$ , respectively. A signal at  $m/z = 771.31$  [M-CO<sub>2</sub> + Na]<sup>+</sup> indicated loss of CO<sub>2</sub>. A 500 MHz <sup>1</sup>H NMR spectrum of 1 in D<sub>2</sub>O and at 293 K showed signals of 38 H atoms, i.e., of all carbon-bound protons. On the basis of <sup>1</sup>H,<sup>1</sup>H-COSY and <sup>1</sup>H,<sup>1</sup>H-ROESY spectra, the chemical constitution of Bo-NCC-1 (1) was deduced. At low field, a singlet was present at 9.15 ppm of the  $\alpha$ -formyl group (H-C(20) at ring A) and the set of

signals between 5 and 6.5 ppm of the vinyl group at C18. Singlets at 1.35, 2.19, 2.22, and at 1.87 ppm were assigned to the methyl groups at C17, C2, C7, and C13, respectively. The methylene protons at C12<sup>1</sup> and C12<sup>2</sup> of the propanoic acid group gave rise to multiplets at 2.26 ppm (H<sub>2</sub>C12<sup>2</sup>) and at 2.64 ppm (H<sub>2</sub>C12<sup>1</sup>). The methylene protons at C3<sup>1</sup> and C3<sup>2</sup> gave multiplets at 2.72 ppm (H<sub>2</sub>-C3<sup>1</sup>), 3.57 ppm, and at 3.72 ppm (H<sub>2</sub>-C3<sup>2</sup>) and coupled with each other. The protons of H<sub>2</sub>-C15 were assigned to the multiplets at 2.74 and 2.86 ppm, both of which coupled with H-C16 at 3.97 ppm. A  $\beta$ -glucopyranosyl unit was identified by <sup>1</sup>H,<sup>1</sup>H-COSY and <sup>1</sup>H,<sup>1</sup>H-ROESY spectra. On the basis of these data, the constitution of *Bo*-NCC-1 (**1**) was deduced as that of a 1-formyl-19-oxo-3<sup>2</sup>-(1- $\beta$ -glucopyranosyl)-O8<sup>4</sup>-desmethyl-16,19-dihydrophyllobilane, a Chl-derived 1-formyl-19-oxobilane (Figure 6).

An ESI mass spectrum of *Bo*-NCC-2 (**2**) (Figure 4) indicated the molecular formula C<sub>34</sub>H<sub>38</sub>N<sub>4</sub>O<sub>7</sub> with pseudomolecular ions at  $m/z$  = 615.30 [M + H]<sup>+</sup>, at  $m/z$  = 637.25 [M + Na]<sup>+</sup> and at  $m/z$  = 653.24 [M + K]<sup>+</sup>. Fragment ions at  $m/z$  = 571.40 [M - CO<sub>2</sub> + H]<sup>+</sup> and  $m/z$  = 593.25 [M - CO<sub>2</sub> + Na]<sup>+</sup>, corresponding to loss of CO<sub>2</sub>, and at  $m/z$  = 448.22 [M - CO<sub>2</sub>-ring D + H]<sup>+</sup>, were also observed. In the 600 MHz <sup>1</sup>H NMR spectrum of **2** in D<sub>2</sub>O at 283 K, signals of 32 of the 38 H atoms could be assigned (i.e., of all carbon-bound H atoms). <sup>1</sup>H,<sup>1</sup>H-COSY and <sup>1</sup>H,<sup>1</sup>H-ROESY spectra were used to derive the chemical constitution of the *Bo*-NCC-2 (**2**) (Figure 5). The

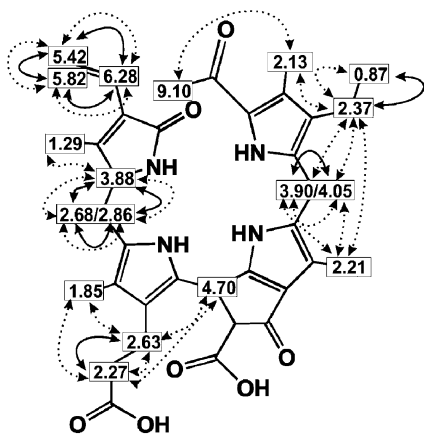


**Figure 5.** Graphical representation of <sup>1</sup>H NMR chemical-shift assignments of signals of carbon-bound H atoms of *Bo*-NCC-2 (**2**) in D<sub>2</sub>O (solid arrows represent COSY correlations, dashed arrows represent ROESY correlations).

characteristic singlet of the aldehyde proton H-C20 appeared at 9.10 ppm. In a 600 MHz NMR spectrum of **2** in H<sub>2</sub>O/D<sub>2</sub>O = 9:1 at 283 K, three additional broad singlets were observed at 7.81, 8.80, and 10.33 ppm of protons bound to pyrrole N-atoms. The signals at 6.28 ppm (dd), at 5.82 ppm (d), and at 5.42 ppm (d) were characteristic of the vinyl group at C18, singlets at 1.29, 1.85, 2.13, and at 2.21 ppm indicated four methyl groups at C17, C13, C2, and C7, respectively. An ethyl group at C3 gave rise to a doublet at 2.37 ppm that coupled with triplet at 0.87 ppm. Multiplets at 2.27 ppm (H<sub>2</sub>C12<sup>2</sup>) and at 2.63 ppm (H<sub>2</sub>C12<sup>1</sup>) characterized the propanoic acid group at ring C. H<sub>2</sub>C15 gave rise to two multiplets at 2.68 and 2.86 ppm, both showing coupling with a multiplet at 3.88 ppm (HC16). HC10 was seen as a signal at 4.70 ppm. On the basis of mass spectrometric and NMR spectroscopic data, *Bo*-NCC-2

(**2**) was deduced to be a 1-formyl-19-oxo-O8<sup>4</sup>-desmethyl-16,19-dihydrophyllobilane (Figure 6).

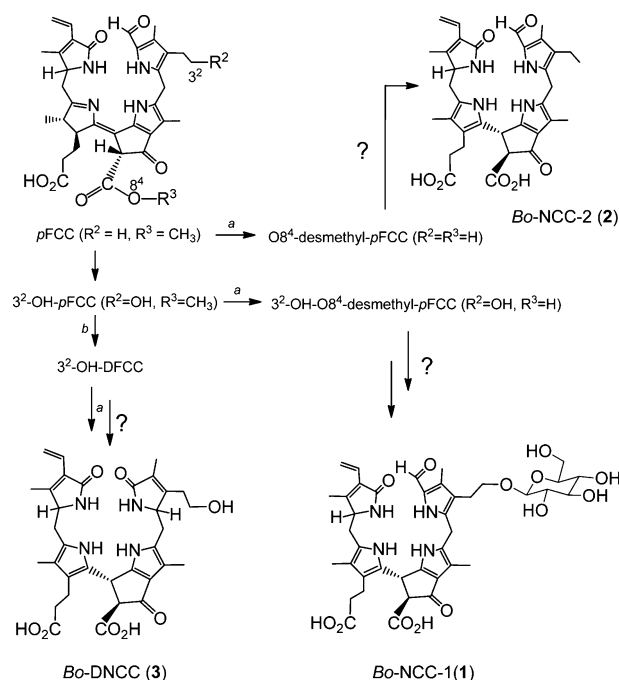


**Figure 6.** Structures of *Bo*-NCC-1 (**1**), *Bo*-NCC-2 (**2**), and *Bo*-DNCC (**3**), the major Chl-catabolites in senescent broccoli, and possible pathways of their formation from pFCC (a, methylsterase; b, deformylating cytochrome). The hypothetical nonenzymatic isomerization of FCCs and of DFCC to NCCs and to DNCC, respectively, is presumed to take place in the vacuole (see Figure 7).

The colorless catabolite *Bo*-DNCC (**3**) was similarly analyzed by an ESI mass spectrum (Figure 4), which showed pseudo molecular ions at  $m/z$  = 619.27 [M + H]<sup>+</sup>, at  $m/z$  = 641.26 [M + Na]<sup>+</sup>, and at  $m/z$  = 657.23 [M + K]<sup>+</sup>, indicating a molecular formula of C<sub>33</sub>H<sub>38</sub>N<sub>4</sub>O<sub>8</sub>. Decarboxylations led to signals at  $m/z$  = 651.23 [M - H-CO<sub>2</sub> + 2K]<sup>+</sup>, 635.22 [M - H-CO<sub>2</sub> + Na + K]<sup>+</sup>, 613.22 [M - CO<sub>2</sub> + K]<sup>+</sup>, and at  $m/z$  = 597.25 [M - CO<sub>2</sub> + Na]<sup>+</sup>. In the 600 MHz <sup>1</sup>H NMR spectrum of **3** in D<sub>2</sub>O and at 283 K, signals of 31 C-bound H atoms could be assigned with the help of <sup>1</sup>H,<sup>1</sup>H-COSY and <sup>1</sup>H,<sup>1</sup>H-ROESY spectra. Signals were not found in the low field, consistent with the absence of a formyl group. A vinyl group at C18 gave rise to a characteristic set of signals between 6.5 and 5 ppm. Four singlets of methyl groups (H<sub>3</sub>C2<sup>1</sup>, H<sub>3</sub>C13<sup>1</sup>, H<sub>3</sub>C17<sup>1</sup>, and H<sub>3</sub>C7<sup>1</sup>) appeared at high field. The methylene protons at C12<sup>1</sup> and C12<sup>2</sup> of the propanoic acid group gave multiplets at 2.13 ppm (H<sub>2</sub>C12<sup>1</sup>) and at 2.45 ppm (H<sub>2</sub>C12<sup>2</sup>). Protons H<sub>2</sub>C3<sup>1</sup> coupled with H<sub>2</sub>C3<sup>2</sup> and H<sub>A</sub>C5 and H<sub>B</sub>C5 coupled with HC4. Similarly, an AB system, due to H<sub>A</sub>C15 and H<sub>B</sub>C15, coupled with HC16. HC10 showed a signal at 4.60 ppm. The mass spectrometric and NMR spectroscopic data established the constitution of the Chl-derived 1,19-dioxobilane **3** as that of a 1,19-dioxo-3<sup>2</sup>-hydroxy-O8<sup>4</sup>-desmethyl-1,4,16,19-tetrahydro-phyllobilane (Figure 6).

The configuration at C10 of the two *Bo*-NCCs **1** and **2** was deduced from the CD spectra to be the same as that of the known natural NCCs, which was tentatively deduced to be (R).<sup>36</sup> The absolute configuration of some other stereocenters could not be independently elucidated. However, **1** and **2** were

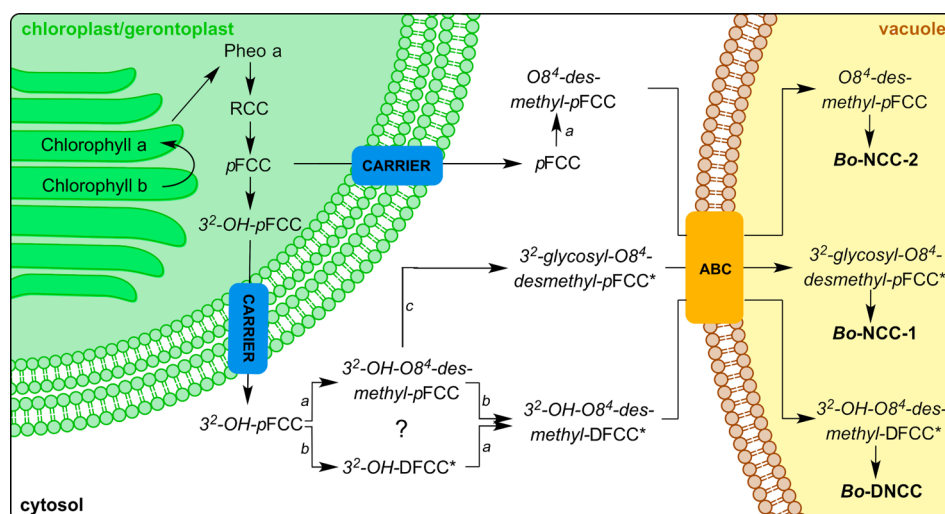


**Figure 7.** Topographical model of Chl-breakdown in senescent leaves of broccoli, according to the “PAO/phylobilin-pathway”.<sup>7,8</sup> The early steps of this pathway take place in the chloroplast/gerontoplast.<sup>7</sup> The model is based on the current tentative view of the subcellular localization of Chl-catabolites,<sup>41</sup> and Chl-catabolic enzymes of the further pathway are specified, based on presumed modifications of breakdown intermediates, as deduced from the structures of colorless Chl-catabolites identified in the present work. Putative catabolites are labeled with asterisk (\*), putative enzyme catalyzed steps are specified by a general label for the enzyme class of a methyl esterase (a), for a deformylating cytochrome (b) and of a glycosidase (c) (see Figure 6 for chemical formulas of the suggested intermediate FCCs and of the nonfluorescent catabolites *Bo-NCC-1* (1), *Bo-NCC-2* (2), and *Bo-DNCC* (3)).

indicated to have the same constitution as two NCCs from oilseed rape (*Brassica napus*), and named *Bn-NCC-2*<sup>34,37</sup> and *Bn-NCC-4*.<sup>38</sup> The structural identity of 1 and 2, on one side, and of *Bn-NCC-2* and *Bn-NCC-4*, on the other,<sup>34</sup> was established by HPL chromatographic comparison (“coinjection” experiments) of these NCCs. As *Bn-NCCs* were shown earlier to be derived from the “primary” fluorescent Chl-catabolite, pFCC<sup>10</sup> (and not from the C1-epimer, *epi-pFCC*<sup>11</sup>), the two *Bo-NCCs* 1 and 2 are also indicated to be derived from pFCC. In a corresponding experiment, *Bo-DNCC* was identified with *At-DNCC-1*, a prominent Chl-derived dioxobilane from *A. thaliana*.<sup>17</sup> Consistent with these data, the colorless Chl-catabolites of broccoli are all derived from pFCC.

## DISCUSSION

Degreening is a characteristic sign of breakdown of chlorophyll (Chl) in higher plants, often associated with senescence.<sup>7,39</sup> In this study, the presence of (colorless) Chl-catabolites was investigated in senescent florets of broccoli (*Brassica oleracea* var. *italica*). Two NCCs (1-formyl-19-oxophyllobilanes) and a DNCC (1,19-dioxophyllobilane) could be identified and were structurally characterized. In the early phase of visual degreening of the broccoli florets (days one and two of storage), the amounts of the three colorless Chl-catabolites recovered roughly comes up for about 30–35% of the Chls that disappear during this time. At later stages (days 5 and 6 of storage), not only the green Chls continue to disappear but Chl-catabolites also fade away (by still unknown processes). So far, nongreen Chl-catabolites have been identified only in one other genuine vegetable, in naturally senescing leaves of spinach (*Spinacia oleracea*).<sup>31,32</sup> A common stereochemical lineage of the catabolites from broccoli with those from oilseed rape (*Brassica napus*)<sup>34</sup> and from *Arabidopsis thaliana*<sup>17</sup> was established, which is consistent with the close phylogenic relationship of the involved *Brassicaceae*.

Similar to observations with wild type *A. thaliana*,<sup>17,38</sup> all three catabolites from broccoli carry a free acid function at C8<sup>2</sup>,

instead of the methyl ester group that is (still) present in their derived common precursor, the “primary” FCC (pFCC).<sup>10</sup> An efficient enzyme catalyzed methyl ester hydrolysis is indicated in broccoli. This finding is in line with the recent discovery of the cytosolic methyl esterase Mes16 in *A. thaliana*,<sup>40</sup> which was shown to be crucial in Chl-breakdown path in this plant. Presumably, in broccoli an analogous methyl esterase exists in the cytosol. The occurrence of the now well characterized less polar *Bo-NCC-2* (2) is notable, which was previously identified provisionally in senescent leaves of *A. thaliana*<sup>38</sup> and of spinach.<sup>31</sup> This observation (in broccoli, *A. thaliana*, etc.) suggests export of the “primary” FCC (pFCC) into the cytosol, where it is a substrate of the methyl esterase that produces O8<sup>4</sup>-desmethyl-pFCC efficiently (the hypothetical precursor of *Bo-NCC-2* (2), Figures 6 and 7).

Identification of *Bo-DNCC* (3), a prominent dioxobilin-type Chl-catabolite in degreened broccoli florets, suggests FCC-deformylation (at C1) to be an important degradation step in broccoli, as was observed in senescent leaves of *A. thaliana*.<sup>17</sup> Thus, similar to the situation in *A. thaliana*, where DNCCs and NCCs were identified,<sup>17</sup> both catabolite lineages occur in broccoli as well. Furthermore, because both hydroxylated DNCC 3 and further glucosylated NCC 1 were found in the extracts of senescent broccoli florets, the enigmatic hydroxylation at the saturated C3<sup>2</sup> position is also indicated to be efficient and to be relevant for both branches of Chl-breakdown. Possibly, this hydroxylation reaction already occurs in the chloroplast, i.e., before export into the cytosol.<sup>7</sup> In contrast, the glycosylation at the OH group at C3<sup>2</sup>, observed in the structure of the polar *Bo-NCC-1* (1), would be considered to occur in the cytosol and at the level of the still elusive hypothetical FCCs (Figures 6 and 7). Chl-breakdown in broccoli thus shows the hallmarks of the PaO/phylobilin pathway,<sup>7,41</sup> and a tentative outline of the Chl-breakdown path in broccoli could be deduced from the structures of the Chl-catabolites found in the degreening florets (see Figures 6 and 7).



In the context of the typical nutritional use of broccoli as a green vegetable, the presence of sizable amounts of colorless Chl-catabolites in the early phase of visual degreening is remarkable. We recently showed NCCs to be excellent antioxidants, such as the ones from apples and pears.<sup>9</sup> Indeed, at present, the physiological effects of the ubiquitous phyllobilanes (NCCs, DNCCs) are unknown that are present in some of our plant-derived nutrition as degradation products of Chl *a*. However, the result with degreening broccoli florets indicates accumulation of such linear tetrapyrroles in this common vegetable, which are also exceptional antioxidants. It will clearly be interesting to learn more about the possible health effects of such colorless Chl-catabolites, as of those that are now known to occur in degreening broccoli florets.

## ■ ASSOCIATED CONTENT

### ■ Supporting Information

Material and methods. Atom numbering of NCCs and of DNCCs used here. Qualitative analyses of the time dependence of the amounts of chlorophyll (Chl) and Chl-catabolites in the raw broccoli plant material during the degreening. HPLC analyses of organic and aqueous phase of the first broccoli extract. Online UV/vis spectra of Bo-NCC-1, Bo-NCC-2, and Bo-NCC-3. CD spectra of Bo-NCC-1, Bo-NCC-2, and Bo-NCC-3. <sup>1</sup>H NMR 600 MHz spectra of Bo-NCC-1, Bo-NCC-2, and Bo-NCC-3. Graphical analysis of homonuclear <sup>1</sup>H,<sup>1</sup>H-ROESY, and COSY correlations of Bo-NCC-1 and Bo-NCC-3. HPLC analyses of Chl-catabolites from broccoli by coinjection experiments. This material is available free of charge via the Internet at <http://pubs.acs.org>.

## ■ AUTHOR INFORMATION

### Corresponding Author

\*Phone: 43-512-507-57700. Fax: +43-512-507-57799. E-mail: [bernhard.kraeutler@uibk.ac.at](mailto:bernhard.kraeutler@uibk.ac.at).

### Funding

Financial support by the Austrian Science Foundation (FWF) project nos. L-472 and I-563) is also gratefully acknowledged.

### Notes

The authors declare no competing financial interest. See formulas and ref 8 for atom-numbering of the chlorophyll catabolites used here.

## ■ ACKNOWLEDGMENTS

We thank Christoph R. Kreutz and Markus Ruetz for measuring NMR-spectra and Clemens Vergeiner, Barbara Enders, and Iris Süssenbacher for technical advice. We thank Stefan Hörtensteiner (University of Zürich) for helpful discussions.

## ■ DEDICATION

Dedicated to the memory of Paula Enders.

## ■ ABBREVIATIONS USED

Chl, chlorophyll; NCC, nonfluorescent chlorophyll catabolite; DNCC, dioxobilane-type chlorophyll catabolite; FCC, fluorescent chlorophyll catabolite; pFCC, "primary" fluorescent chlorophyll catabolite; sFCC, "secondary" fluorescent chlorophyll catabolite; RCC, red chlorophyll catabolite; HPLC, high performance liquid chromatography; UV/vis, ultraviolet/visible absorption; CD, circular dichroism; <sup>1</sup>H NMR, proton nuclear

magnetic resonance; ESI-MS, electrospray ionization mass spectrometry

## ■ REFERENCES

- (1) Lim, P. O.; Kim, H. J.; Nam, H. G. Leaf Senescence. *Annu. Rev. Plant Biol.* **2007**, *58*, 115–136.
- (2) Hörtensteiner, S.; Lee, D. W. Chlorophyll Catabolism and Leaf Coloration. In *Senescence Processes in Plants*; Gan, S., Ed.; Blackwell Publishing Ltd: Oxford, UK, 2007; p 12.
- (3) Barry, C. S. The Stay-Green Revolution: Recent Progress in Deciphering the Mechanisms of Chlorophyll Degradation in Higher Plants. *Plant Sci.* **2009**, *176*, 325–333.
- (4) Kräutler, B.; Jaun, B.; Bortlik, K.; Schellenberg, M.; Matile, P. On the Enigma of Chlorophyll Degradation—The Constitution of a Secoporphinoid Catabolite. *Angew. Chem., Int. Ed.* **1991**, *30*, 1315–1318.
- (5) Kräutler, B. Chlorophyll Breakdown and Chlorophyll Catabolites in Leaves and Fruit. *Photochem. Photobiol. Sci.* **2008**, *7*, 1114–1120.
- (6) Moser, S.; Müller, T.; Oberhuber, M.; Kräutler, B. Chlorophyll Catabolites—Chemical and Structural Footprints of a Fascinating Biological Phenomenon. *Eur. J. Org. Chem.* **2009**, 21–31.
- (7) Hörtensteiner, S.; Kräutler, B. Chlorophyll Breakdown in Higher Plants. *Biochim. Biophys. Acta, Bioenerg.* **2011**, *1807*, 977–988.
- (8) Kräutler, B. Phyllobilins—The Abundant Tetrapyrrolic Catabolites of the Green Plant Pigment Chlorophyll. *Chem. Soc. Rev.* **2014**, *43*, 6227–6238.
- (9) Müller, T.; Ulrich, M.; Ongania, K.-H.; Kräutler, B. Colourless Tetrapyrrolic Chlorophyll Catabolites Found in Ripening Fruit are Effective Antioxidants. *Angew. Chem., Int. Ed.* **2007**, *46*, 8699–8702.
- (10) Mühlecker, W.; Ongania, K. H.; Kräutler, B.; Matile, P.; Hörtensteiner, S. Tracking Down Chlorophyll Breakdown in Plants: Elucidation of the Constitution of a 'Fluorescent' Chlorophyll Catabolite. *Angew. Chem., Int. Ed.* **1997**, *36*, 401–404.
- (11) Mühlecker, W.; Kräutler, B.; Moser, D.; Matile, P.; Hörtensteiner, S. Breakdown of Chlorophyll: A Fluorescent Chlorophyll Catabolite from Sweet Pepper (*Capsicum annum*). *Helv. Chim. Acta* **2000**, *83*, 278–286.
- (12) Kräutler, B.; Hörtensteiner, S. Chlorophyll Breakdown—Chemistry, Biochemistry and Biology. In *Handbook of Porphyrin Science*; Ferreira, G. C., Kadish, K. M., Smith, K. M., Guillard, R., Ed.; World Scientific Publishing, Hackensack, NJ, 2013; Vol. 28, p 117.
- (13) Losey, F. G.; Engel, N. Isolation and Characterization of a Urobilinogenoid Chlorophyll Catabolite from *Hordeum vulgare*. *J. Biol. Chem.* **2001**, *276*, 8643–8647.
- (14) Scherl, M.; Müller, T.; Kräutler, B. Chlorophyll Catabolites in Senescent Leaves of the Lime Tree (*Tilia cordata*). *Chem. Biodiversity* **2012**, *9*, 2605–2617.
- (15) Oberhuber, M.; Berghold, J.; Kräutler, B. Chlorophyll Breakdown by a Biomimetic Route. *Angew. Chem., Int. Ed.* **2008**, *47*, 3057–3061.
- (16) Müller, T.; Rafelsberger, M.; Vergeiner, C.; Kräutler, B. A Dioxobilane as Product of a Divergent Path of Chlorophyll Breakdown in Norway Maple. *Angew. Chem., Int. Ed.* **2011**, *50*, 10724–10727.
- (17) Christ, B.; Süssenbacher, I.; Moser, S.; Bichsel, N.; Egert, A.; Müller, T.; Kräutler, B.; Hörtensteiner, S. Cytochrome P450 CYP89A9 is Involved in the Formation of Major Chlorophyll Catabolites During Leaf Senescence in *Arabidopsis thaliana*. *Plant Cell* **2013**, *25*, 1868–1880.
- (18) Fukasawa, A.; Suzuki, Y.; Terai, H.; Yamauchi, N. Effects of Postharvest Ethanol Vapor Treatment on Activities and Gene Expression of Chlorophyll Catabolic Enzymes in Broccoli Florets. *Postharvest Biol. Technol.* **2010**, *55*, 97–102.
- (19) King, G. A.; O'Donoghue, E. M. Unravelling Senescence: New Opportunities for Delaying the Inevitable in Harvested Fruit and Vegetables. *Trends Food Sci. Technol.* **1995**, *6*, 385–389.
- (20) Gapper, N. E.; Coupe, S. A.; McKenzie, M. J.; Sinclair, B. K.; Lill, R. E.; Jameson, P. E. Regulation of Harvest-induced Senescence in Broccoli (*Brassica oleracea* var. *italica*) by Cytokinin, Ethylene and Sucrose. *J. Plant Growth Regul.* **2005**, *24*, 153–165.

- (21) Van Loey, A.; Ooms, V.; Weemaes, C.; Van den Broeck, I.; Ludikhuyze, L.; Indrawati, Denys, S.; Hendrickx, M. Thermal and Pressure–Temperature Degradation of Chlorophyll in Broccoli (*Brassica oleracea* L. *italica*) juice: A Kinetic Study. *J. Agric. Food Chem.* **1998**, *46*, 5289–5294.
- (22) Yamauchi, N.; Harada, K.; Watada, A. E. In Vitro Chlorophyll Degradation in Stored Broccoli (*Brassica oleracea* L. var. *italica* Plen.) Florets. *Postharvest Biol. Technol.* **1997**, *12*, 239–245.
- (23) Büchert, A. M.; Civello, P. M.; Martínez, G. A. Chlorophyllase versus Pheophytinase as Candidates for Chlorophyll Dephytilation during Senescence of Broccoli. *J. Plant Physiol.* **2011**, *168*, 337–343.
- (24) Gomez-Lobato, M. E.; Civello, P. M.; Martínez, G. A. Effects of Ethylene, Cytokinin and Physical Treatments on *BoPaO* Gene Expression of Harvested Broccoli. *J. Sci. Food Agric.* **2012**, *92*, 151–158.
- (25) Chen, L. F. O.; Lin, C. H.; Kelkar, S. M.; Chang, Y. M.; Shaw, J. F. Transgenic Broccoli (*Brassica oleracea* var. *italica*) with Antisense Chlorophyllase (BoCLH1) Delays Postharvest Yellowing. *Plant Sci.* **2008**, *174*, 25–31.
- (26) Aiamla-or, S.; Kaewsuksaeng, S.; Shigyo, M.; Yamauchi, N. Impact of UV-B Irradiation on Chlorophyll Degradation and Chlorophyll-Degrading Enzyme Activities in Stored Broccoli (*Brassica oleracea* L. *italica* Group) Florets. *Food Chem.* **2010**, *120*, 645–651.
- (27) Funamoto, Y.; Yamauchi, N.; Shigyo, M. Involvement of Peroxidase in Chlorophyll Degradation in Stored Broccoli (*Brassica oleracea* L.) and Inhibition of the Activity by Heat Treatment. *Postharvest Biol. Technol.* **2003**, *28*, 39–46.
- (28) Zhang, X. L.; Zhang, Z. Q.; Li, J.; Wu, L. J.; Guo, J. Y.; Ouyang, L. Q.; Xia, Y. Y.; Huang, X. M.; Pang, X. Q. Correlation of Leaf Senescence and Gene Expression/Activities of Chlorophyll Degradation Enzymes in Harvested Chinese Flowering Cabbage (*Brassica rapa* var. *parachinensis*). *J. Plant Physiol.* **2011**, *168*, 2081–2087.
- (29) Gomez, F.; Fernandez, L.; Gergoff, G.; Guamet, J. J.; Chaves, A.; Bartoli, C. G. Heat Shock Increases Mitochondrial H<sub>2</sub>O<sub>2</sub> Production and Extends Postharvest Life of Spinach Leaves. *Postharvest Biol. Technol.* **2008**, *49*, 229–234.
- (30) Nath, A.; Bagchi, B.; Misra, L. K.; Deka, B. C. Changes in Post-Harvest Phytochemical Qualities of Broccoli Florets During Ambient and Refrigerated Storage. *Food Chem.* **2011**, *127*, 1510–1514.
- (31) Berghold, J.; Breuker, K.; Oberhuber, M.; Hörtensteiner, S.; Kräutler, B. Chlorophyll Breakdown in Spinach: On the Structure of Five Nonfluorescent Chlorophyll Catabolites. *Photosynth. Res.* **2002**, *74*, 109–119.
- (32) Oberhuber, M.; Berghold, J.; Mühlecker, W.; Hörtensteiner, S.; Kräutler, B. Chlorophyll Breakdown—On a Nonfluorescent Chlorophyll Catabolite from Spinach. *Helv. Chim. Acta* **2001**, *84*, 2615–2627.
- (33) Porra, R. J.; Thompson, W. A.; Kriedemann, P. E. Determination of Accurate Extinction Coefficients and Simultaneous-Equations for Assaying Chlorophyll-a and Chlorophyll-b Extracted with 4 Different Solvents—Verification of the Concentration of Chlorophyll Standards by Atomic-Absorption Spectroscopy. *Biochim. Biophys. Acta* **1989**, *975*, 384–394.
- (34) Mühlecker, W.; Kräutler, B. Breakdown of chlorophyll: Constitution of Nonfluorescing Chlorophyll Catabolites from Senescent Cotyledons of the Dicot Rape. *Plant Physiol. Biochem.* **1996**, *34*, 61–75.
- (35) Kräutler, B.; Jaun, B.; Amrein, W.; Bortlik, K.; Schellenberg, M.; Matile, P. Breakdown of Chlorophyll—Constitution of a Secoporphinoid Chlorophyll Catabolite Isolated from Senescent Barley Leaves. *Plant Physiol. Biochem.* **1992**, *30*, 333–346.
- (36) Oberhuber, M.; Berghold, J.; Breuker, K.; Hörtensteiner, S.; Kräutler, B. Breakdown of Chlorophyll: A Nonenzymatic Reaction Accounts for the Formation of the Colorless ‘Nonfluorescent’ Chlorophyll Catabolites. *Proc. Natl. Acad. Sci. U. S. A.* **2003**, *100*, 6910–6915.
- (37) Mühlecker, W.; Kräutler, B.; Ginsburg, S.; Matile, P. Breakdown of Chlorophyll—A Tetrapyrrolic Chlorophyll Catabolite from Senescent Rape Leaves. *Helv. Chim. Acta* **1993**, *76*, 2976–2980.
- (38) Pružinska, A.; Tanner, G.; Aubry, S.; Anders, I.; Moser, S.; Müller, T.; Ongania, K.-H.; Kräutler, B.; Youn, J.-Y.; Liljegren, S. J.; Hörtensteiner, S. Chlorophyll Breakdown in Senescent *Arabidopsis* Leaves. Characterization of Chlorophyll Catabolites and of Chlorophyll Catabolic Enzymes Involved in the Degreening Reaction. *Plant Physiol.* **2005**, *139*, 52–63.
- (39) Kräutler, B.; Matile, P. Solving the Riddle of Chlorophyll Breakdown. *Acc. Chem. Res.* **1999**, *32*, 35–43.
- (40) Christ, B.; Schelbert, S.; Aubry, S.; Süßenbacher, I.; Müller, T.; Kräutler, B.; Hörtensteiner, S. MES16, a Member of the Methyl Esterase Protein Family, Specifically Demethylates Fluorescent Chlorophyll Catabolites During Chlorophyll Breakdown in *Arabidopsis*. *Plant Physiol.* **2012**, *158*, 628–641.
- (41) Hörtensteiner, S. Update on the biochemistry of chlorophyll breakdown. *Plant Mol. Biol.* **2013**, *82*, 505–517.